

Research Article

Optimization of Forging Process Parameters and Prediction Model of Residual Stress of Ti-6Al-4V Alloy

Xiurong Fang ¹, Liu Liu ¹, Jia Lu,² and Yang Gao³

¹School of Mechanical Engineering, Xi'an University of Science and Technology, Xi'an 710054, China

²Wuhan Huazhong Numerical Control Co.,Ltd., Wuhan 430223, China

³CRRC Qishuyan Institute Co.,Ltd., Changzhou 213011, China

Correspondence should be addressed to Xiurong Fang; fangxr098@163.com

Received 23 June 2021; Accepted 2 September 2021; Published 15 September 2021

Academic Editor: F.H. Samuel

Copyright © 2021 Xiurong Fang et al. This is an open access article distributed under the Creative Commons Attribution License, which permits unrestricted use, distribution, and reproduction in any medium, provided the original work is properly cited.

Nonisothermal forging is an efficient plastic forming method for titanium alloys, but at the same time, it can produce large and uneven residual stress, which seriously affects the service life of components. In order to quantitatively analyze the influence of forging process parameters on the residual stress of Ti-6Al-4V alloy forgings, a numerical model was first established and optimized in combination with experiments. Then, the effects of deformation temperature, deformation degree, and deformation speed on the residual stress of forgings were analyzed by orthogonal test, and the optimal combination of forging process parameters was obtained. Finally, the multiple regression analysis was employed to propose multivariate regression models for the prediction of the average equivalent residual stress. Results show that the prediction model can be used for predicting the residual stress of Ti-6Al-4V alloy forgings with a higher reliability.

1. Introduction

Titanium and its alloys are often selected for use in high-value structural components in a number of applications due to their high specific strength, relatively low density, excellent corrosion resistance, and fatigue resistance [1–3]. Aerospace industry accounts for the majority of titanium consumption in the world, and more than 80% of titanium is used to produce a variety of alloys, among which Ti-6Al-4V is the most widespread variant [4]. In order to ensure the mechanical properties and dimensional stability of related parts, nonisothermal forging is usually used to process them [5]. Nonisothermal forging is a deformation method with high strain rate, which can greatly improve the mechanical properties of titanium alloys. However, residual stress often occurs in the forging process due to thermal conductivity, high deformation resistance, and narrow forging temperature range of Ti-6Al-4V alloy [6, 7]. In the process of machining, residual stress will cause the forging to deform and even crack, which reduces the qualified rate [8, 9]. In the service process, residual stress will affect the mechanical

properties of components and reduce their service life [10, 11]. Therefore, it is necessary to reduce the residual stress of Ti-6Al-4V alloy forgings in the forging process.

At present, many researchers have conducted a lot of studies on reducing residual stress. Araghchi et al. [12] studied the effect of different concentrations of quenchant on the residual stress of the alloy. The results showed that quenching in 15% polymer solution and aging at 190°C for 12 h could reduce the residual stress, but the mechanical properties of the alloy decreased. Robinson et al. [13] analyzed the influence of quenching temperature on residual stress, and the results showed that quenching had little effect on residual stress when the quenching temperature was low, but the residual stress of the alloy could be reduced when the water temperature was above 100°C. Ya Bo Dong et al. [14] analyzed the effect of heat treatment on the residual stress of forged plate and improved the balance of mechanical properties and residual stress of forged plate by changing the heat treatment process parameters. It can be seen that most researchers reduce the residual stress of forgings by adjusting the heat treatment process parameters. However,

as far as the present technology is concerned, it is impossible to completely eliminate the residual stress of forgings by heat treatment [15]. In addition, it was found that the qualified rate of a certain type of blade is increased by 20%–30% after heat treatment and the adjustment of cutting process parameters, but there are still a lot of scrapped products due to deformation, and the total qualified rate is only 70%. After the analysis of the scrapped products, it was found that forging process parameters have a great influence on the residual stress of forgings. In addition, Karunathilaka et al. [16] analyzed the influence of lubrication and forging load on residual stress and found that there is a positive relationship between the forging load and residual stress. Ameli et al. [17] investigated the effects of process parameters such as workpiece and die geometries, percentage of deformation, and workpiece motions on residual stresses. Ye Zhang et al. [18] analyzed the influences of different process parameters on residual stress during turbine disc hot die forging by numerical simulation. They all found that the key forging process parameters have a considerable influence on the residual stress of forgings [19]. Therefore, it is of great practical significance to reduce the residual stress and improve the distribution of residual stress in forgings by optimizing the forging process parameters.

In this paper, the residual stress of Ti-6Al-4V alloy forgings under different forging processes (deformation temperature, deformation degree, and deformation speed) were analyzed based on the finite element method, and the optimal combination of forging process parameters was obtained through the orthogonal test. Then, a mathematical model for predicting the average equivalent residual stress was established by regression analysis of the simulation data, which can provide effective guidance for the actual forging process.

2. Calculation Model

2.1. Establishment of the Simulation Model. In the process of numerical simulation, the blank is defined as an elastic-plastic body because of the elastoplastic transformation of materials while the dies are defined as a rigid body. In addition, due to the temperature difference between the blank and the dies, as well as between the blank and the air, the simulation control parameters such as the heat conduction between the blank and the dies, the heat convection between the blank and the air, and the heat radiation of the blank should be considered when establishing the simulation model. The heat transfer of forgings is shown in Figure 1 [20].

The geometric models of the upper and lower dies and the forging blank were established using three-dimensional drawing software, as shown in Figure 2(a). The size of the forging blank is $\Phi 60\text{ mm} \times 100\text{ mm}$. Considering the lengthwise symmetrical characteristic and the complexity of the elastic-plastic finite element analysis, one fourth of the forging billet was taken for analysis, and the finite element model is shown in Figure 2(b).

The accuracy of the simulation results is affected by the control parameters. Therefore, in order to obtain more accurate control parameters, this paper combines

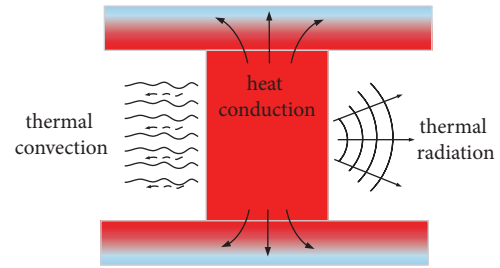


FIGURE 1: Heat transfer of forgings.

physical experiments and numerical simulation to analyze the residual stress of Ti-6Al-4V alloy forgings after nonisothermal forging [21]. Firstly, the forging experiment and residual stress detection test were carried out to obtain the residual stress of the forging. Two sets of different forging process parameters were selected (one set is deformation temperature 975°C , deformation degree 50%, and deformation speed 10 mm/s, and the other set is deformation temperature 925°C , deformation degree 50%, and deformation speed 20 mm/s). Five experimental samples were taken under each set of process parameters, and the average value of residual stress was taken as the final result. The specific experimental process is shown in Figure 3 [20]. Then, the corresponding numerical simulation was carried out. Based on the forging residual stress measured in physical experiment, the error between experimental results and simulation results was analyzed. Finally, the simulation control parameters were adjusted until the residual stress values of the simulation are as close as possible to the experimental measurements. The final simulation control parameters are shown in Table 1.

2.2. Results' Analysis. In order to intuitively show the distribution of residual stress of Ti-6Al-4V alloy forgings under nonisothermal forging, a set of forging process parameters (deformation temperature 925°C , deformation degree 50%, and deformation speed 100 mm/s) was selected for simulation analysis according to the engineering practice, and the result is shown in Figure 4.

In order to further reveal the distribution characteristics of residual stress, 11 tracking points with a spacing of 5 mm were selected from the upper surface to the lower surface along the central axis of the forging. The distribution of the residual stress at the tracking points along the XYZ direction is shown in Figure 5. It can be seen from Figure 5 that the distribution characteristics of the residual stress in the X and Y directions of the forging are basically similar, which are symmetrical but uneven about the center of the axis. In the direction of the central axis, the residual stress on the surface of the forging is tensile stress while the center is compressive stress. From the surface to the core, the tensile stress is transformed into compressive stress. The residual stress in Z direction is less than that in X and Y directions, and the distribution is more uniform.

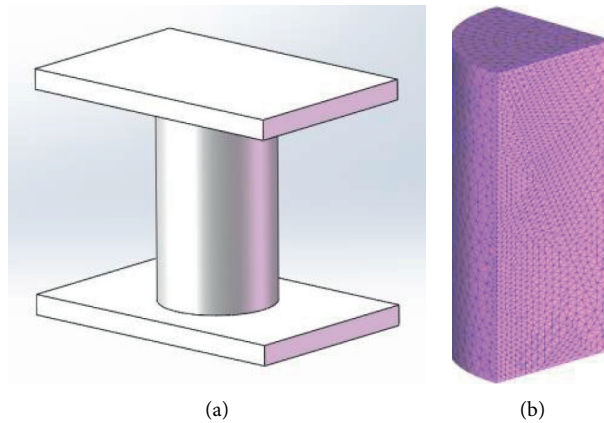


FIGURE 2: Simulation model of forging. (a) Geometric model. (b) Finite element model.

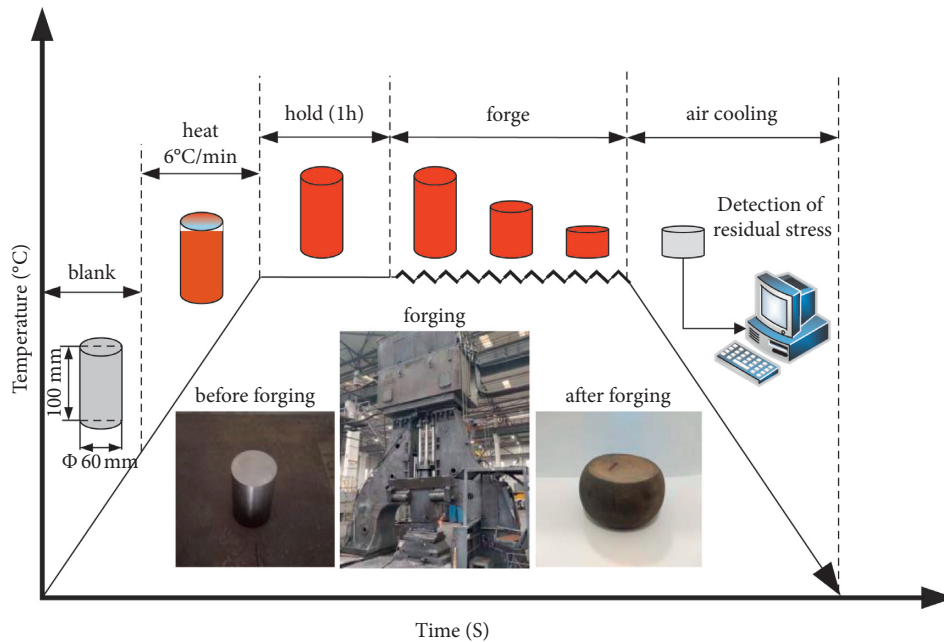


FIGURE 3: Physical experiment process [20].

TABLE 1: Forging simulation parameters.

Simulation parameters	Value	Simulation parameters	Value
Environment temperature (°C)	20	Thermal radiation rate	0.7
Die temperature (°C)	300	Step (mm)	0.25
Friction coefficient	0.3	Thermal convection coefficient ($N s^{-1} mm^{-1} °C^{-1}$)	0.02
Thermal conductivity of the bottom die ($N s^{-1} mm^{-1} °C^{-1}$)	1	Thermal conductivity of the forging ($N s^{-1} mm^{-1} °C^{-1}$)	5

3. Optimization of Forging Process Parameters Based on Orthogonal Test

3.1. *Orthogonal Test Factors.* In nonisothermal forging, it is necessary to select the appropriate forging process parameters for analysis to correctly guide the actual processing. According to the characteristics of Ti-6Al-4V alloy,

such as transformation temperature (985°C), forging method, allowable forging deformation degree, and speed, the deformation temperature, deformation degree, and deformation speed were determined as the key process parameters. Through further research, it was found that these parameters have a great influence on the residual stress of forgings [20].

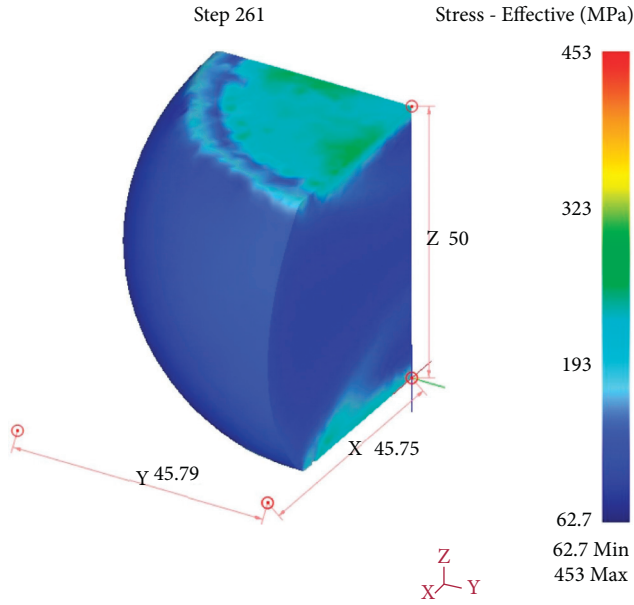


FIGURE 4: Distribution of equivalent residual stress.

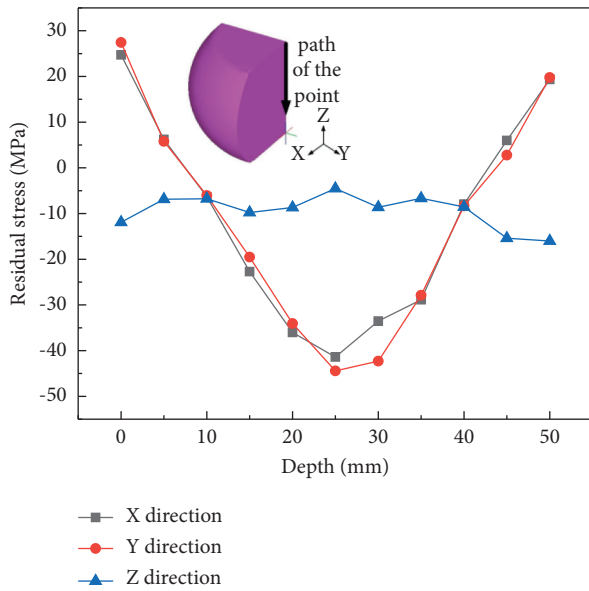


FIGURE 5: Distribution of residual stress in XYZ direction of the forging at different depths.

3.2. Orthogonal Test Schemes. Taking deformation temperature, deformation degree, and deformation speed as test factors, five levels are set for each factor, as shown in Table 2.

In accordance with the $L_{25}(5^3)$ orthogonal table, 25 sets of orthogonal test schemes are established, as shown in Table 3, where T is deformation temperature, D is deformation degree, S is deformation speed, and σ is the average equivalent residual stress.

3.3. Orthogonal Test Results. Range analysis is usually used to analyze the results of an orthogonal test [22]. It can be described as shown in the following equation [23]:

$$K_i = \frac{1}{n} \sum_{j=1}^n E_j, \quad (1)$$

$$R = K_{i_{\max}} - K_{i_{\min}}, \quad (2)$$

where E_j is the value of a certain factor, K_i is the average of each factor, and R is the range and used to estimate design variable sensitivities [24]. In general, the greater the K_i value, the higher the indicator values under this level, and if the value of R is larger, the factor value would be more influential [25]. The range analysis of the orthogonal test results was calculated according to equations (1) and (2), as shown in Table 4

It can be clearly found from Table 4 that the primary and secondary relationship of factors affecting the residual stress of the forging is deformation temperature, deformation degree, and deformation speed. And, their contribution rates to the residual stress of forgings are 56%, 28%, and 16%, respectively. Comparing the minimum values of $K_1 \sim K_5$ under each factor, the optimal combination of process parameters with the smallest residual stress can be determined as deformation temperature 1025 °C, deformation degree 30%, and deformation speed 1000 mm/s.

3.4. Numerical Simulation of Optimized Process Parameters. The forging process of Ti-6Al-4V alloy was simulated under the optimal process parameters of deformation temperature 1025 °C, deformation degree 30%, and deformation speed 1000 mm/s. The results are shown in Figure 6. It can be seen from Figure 6 that the residual stress of the forgings under the optimal combination of process parameters basically belongs to normal distribution, without obvious stress concentration, and the distribution is relatively uniform. This is because when the deformation temperature (1025 °C) far exceeds the transformation temperature of Ti-6Al-4V alloy (985°C), the forging is completed in the β single-phase region. The plastic forming ability of the forgings is significantly improved and the deformation resistance is greatly reduced, which greatly improves the deformation uniformity. Furthermore, when the deformation degree is 30%, the main softening mechanism of Ti-6Al-4V alloy forgings is dynamic recovery. The residual stress of the forgings decreases sharply during the recovery stage. In addition, the deformation temperature is high and the degree of deformation is small at this time, which reduces the heat converted and weakens the thermal effect of metal deformation, thereby greatly reducing the residual stress of the forging and improving the distribution of the residual stress.

However, when the forging temperature is above the β -transition temperature, there are a lot of coarse β -grains in the forgings. The coarser the grain, the more uneven the plastic deformation and the greater the internal stress concentration. Moreover, the coarse grains reduce the chance of crisscross between grains, which will be conducive to the propagation and development of cracks, and the strength and toughness will become worse. So, the mechanical properties will be reduced. Therefore, for the parts

TABLE 2: Level table of orthogonal test factors.

Levels	Factors		
	T (deformation temperature ($^{\circ}\text{C}$))	D (deformation degree (%))	S (deformation speed ($\text{mm}\cdot\text{s}^{-1}$))
1	925	30	10
2	950	40	50
3	975	50	100
4	1000	60	500
5	1025	70	1000

TABLE 3: Orthogonal test schemes.

Test no.	Factors			Test index σ (MPa)
	T	D	S	
1	1 (925)	1 (30)	1 (10)	14.5
2	1 (925)	2 (40)	2 (50)	18.3
3	1 (925)	3 (50)	3 (100)	18.1
4	1 (925)	4 (60)	4 (500)	17.4
5	1 (925)	5 (70)	5 (1000)	18.9
6	2 (950)	1 (30)	2 (50)	12.1
7	2 (950)	2 (40)	3 (100)	15.3
8	2 (950)	3 (50)	4 (500)	15.4
9	2 (950)	4 (60)	5 (1000)	14.3
10	2 (950)	5 (70)	1 (10)	20.8
11	3 (975)	1 (30)	3 (100)	11.8
12	3 (975)	2 (40)	4 (500)	11.4
13	3 (975)	3 (50)	5 (1000)	11.8
14	3 (975)	4 (60)	1 (10)	19.7
15	3 (975)	5 (70)	2 (50)	18.5
16	4 (1000)	1 (30)	4 (500)	9.79
17	4 (1000)	2 (40)	5 (1000)	9.04
18	4 (1000)	3 (50)	1 (10)	10.7
19	4 (1000)	4 (60)	2 (50)	10.7
20	4 (1000)	5 (70)	3 (100)	11
21	5 (1025)	1 (30)	5 (1000)	8.04
22	5 (1025)	2 (40)	1 (10)	8.58
23	5 (1025)	3 (50)	2 (50)	9.22
24	5 (1025)	4 (60)	3 (100)	8.83
25	5 (1025)	5 (70)	4 (500)	9.2

TABLE 4: Influence analysis of parameters on the residual stress.

Parameters	T	D	S
K_1	17.440	11.246	14.856
K_2	15.580	12.524	13.764
K_3	14.640	13.044	13.006
K_4	10.246	14.186	12.638
K_5	8.774	15.680	12.416
R	8.666	4.432	2.440
Sorting	1	2	3

that require high-dimensional stability but not too much mechanical properties, this combination of forging parameters can be used as an effective guide.

4. Development of Prediction Model

4.1. Regression Model and Calculation. In order to further quantitatively analyze the relationship between the key forging process parameters and the average equivalent

residual stress, regression analysis was carried out on the simulation data to find the mapping relationship between them, so as to determine a mathematical model that can effectively predict the average equivalent residual stress of the forgings and provide effective guidance for the actual forging process [26].

Based on Table 2 and the analysis results of Table 4, the change curve of the average equivalent residual stress under each factor is shown in Figure 7.

It can be seen from Figure 7 that when the deformation temperature exceeds the transformation temperature (985°C) of Ti-6Al-4V alloy, the average equivalent residual stress of forgings decreases sharply. However, there is a linear relationship between the deformation temperature and the average equivalent residual stress in the two different temperature ranges above and below the transformation temperature. In addition, when the deformation degree is between 40% and 70%, there is a linear relationship between the deformation degree and the average equivalent residual stress. And, when the deformation velocity is between

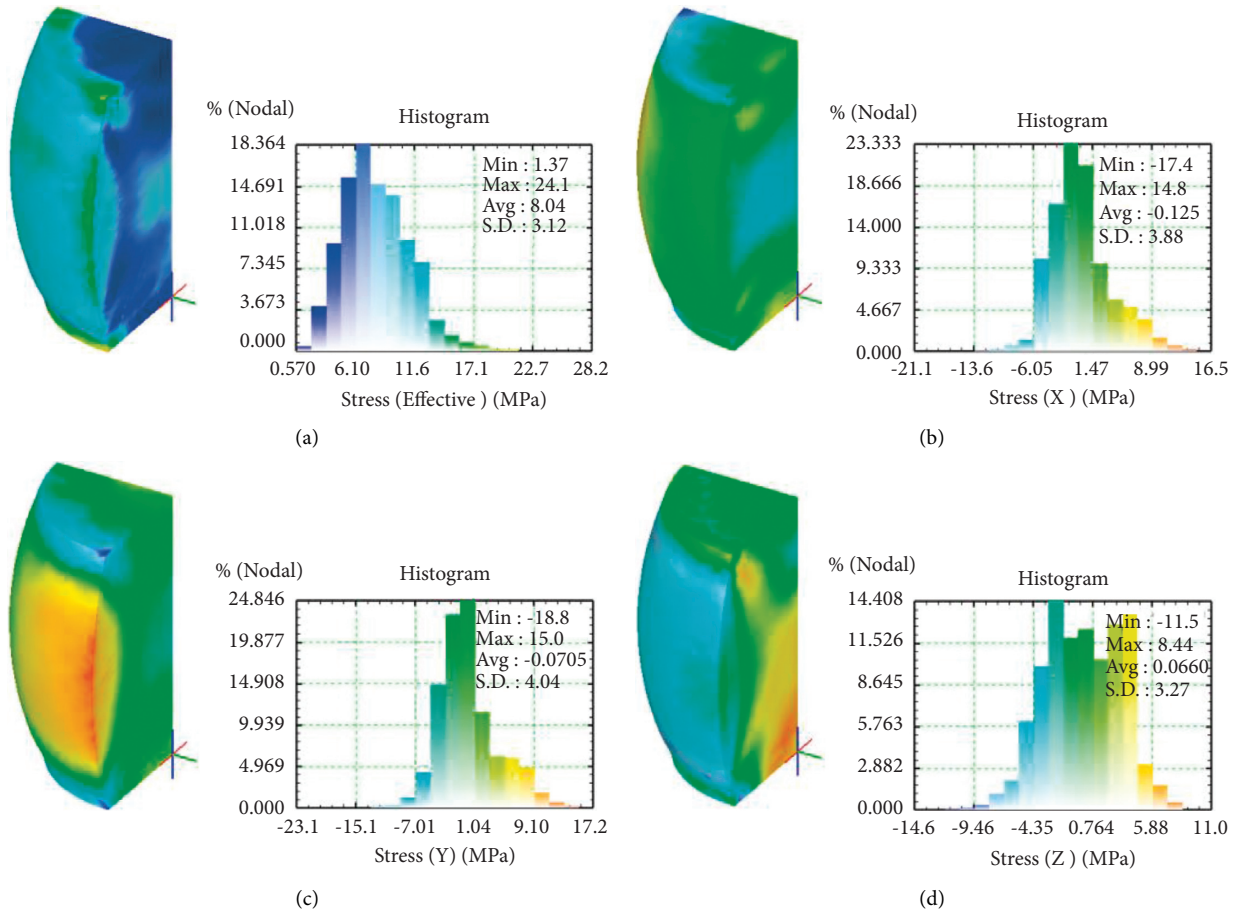


FIGURE 6: Distribution of forging residual stress under the optimal process parameters. (a) Equivalent residual stress. (b) Residual stress in the X direction. (c) Residual stress in the Y direction. (d) Residual stress in the Z direction.

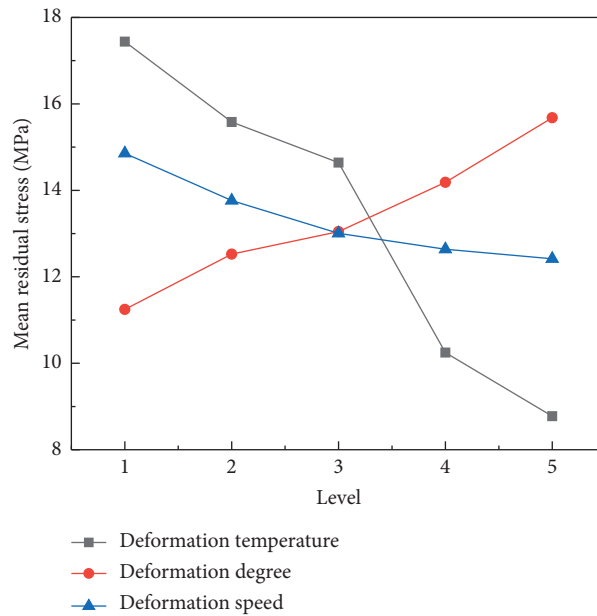


FIGURE 7: Variation curve of average equivalent residual stress under each factor.

TABLE 5: Regression analysis of sample data (925°C–980°C).

Sample	T	D	S	σ (MPa)
1	925	40	100	18.5
2	925	60	500	17.4
3	925	50	100	18
4	925	60	100	18.5
5	950	50	100	15.3
6	950	60	1000	14.3
7	950	70	500	15.5
8	950	50	300	14.9
9	950	60	500	14.6
10	950	40	1000	14.4
11	950	60	300	15.1
12	950	50	1000	14.4
13	950	40	100	15.3
14	975	40	500	11.4
15	975	40	100	12.2
16	975	50	100	12.6
17	975	70	100	13.5
18	975	40	1000	11.1
19	975	50	1000	11.8
20	975	70	300	12.6
21	980	40	300	11.4
22	980	50	100	12.1
23	980	40	1000	10.5
24	980	50	500	11.5
25	980	70	100	12.4

TABLE 6: Regression analysis of sample data (990°C–1025°C).

Sample	T	D	S	σ (MPa)
1	990	40	100	10.2
2	990	50	300	10.7
3	990	60	500	10.6
4	990	40	300	10.4
5	990	40	1000	9.61
6	990	50	500	10.8
7	1000	40	300	9.63
8	1000	60	1000	9.79
9	1000	70	500	10.6
10	1000	40	1000	9.04
11	1000	70	100	11
12	1010	40	500	8.82
13	1010	40	300	8.99
14	1010	60	100	9.5
15	1010	70	300	10
16	1010	50	500	9.3
17	1010	60	300	9.33
18	1025	60	300	8.35
19	1025	70	100	9.19
20	1025	60	100	8.83
21	1025	70	500	9.2
22	1025	40	100	8.2
23	1025	50	100	8.93
24	1025	50	300	8.3
25	1025	40	500	8.1

100 mm/s and 1000 mm/s, the relationship between the deformation velocity and the average equivalent residual stress is basically linear.

Based on the above characteristics, the deformation temperature was divided into two intervals. Then, regression model I was established by taking deformation temperature, deformation degree, and deformation velocity as independent variables and average equivalent residual stress as dependent variable. At the same time, considering the difference in the order of magnitude of the selected parameters, the logarithmic transformation was carried out to establish regression model II.

Set the average equivalent residual stress as σ (MPa), deformation temperature as t (°C), deformation degree as d (%), and deformation speed as s (mm/s), among which $t \in [925, 980] \cup [990, 1025]$, $d \in [40, 70]$, and $s \in [100, 1000]$.

The two regression models were as follows:

$$\text{Model I: } \begin{cases} \sigma = a_{10}t + a_{11}d + a_{12}s + C_1 & (925 \leq t \leq 980) \\ \sigma = a_{20}t + a_{21}d + a_{22}s + C_2 & (990 \leq t \leq 1025) \end{cases},$$

$$\text{Model II: } \begin{cases} \sigma = e^{(a_{10}t + a_{11}d + a_{12}s + C_1)} & (925 \leq t \leq 980) \\ \sigma = e^{(a_{20}t + a_{21}d + a_{22}s + C_2)} & (990 \leq t \leq 1025) \end{cases} \quad (3)$$

Fifty sets of sample data were obtained using the modified finite element model of residual stress of Ti-6Al-4V alloy forgings under nonisothermal forging. Among them, 25 sets of sample data with deformation temperature between 925°C and 980°C are shown in Table 5, and the other 25 sets of sample data with deformation temperature between 990°C and 1025°C are shown in Table 6.

Based on the sample data in Tables 5 and 6, the mathematical analysis software was used to analyze and

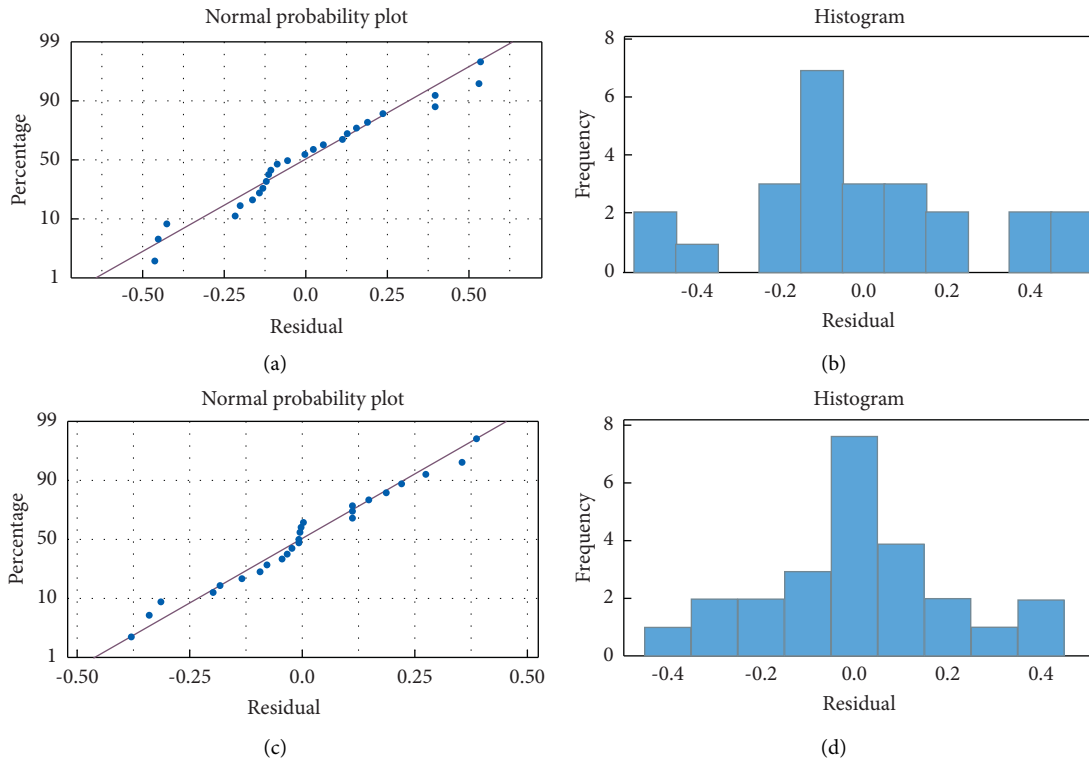


FIGURE 8: Analysis results of model I. (a) Normal probability plot ($925 \leq (t) \leq 980$). (b) Histogram ($925 \leq (t) \leq 980$). (c) Normal probability plot ($990 \leq (t) \leq 1025$). (d) Histogram ($990 \leq (t) \leq 1025$).

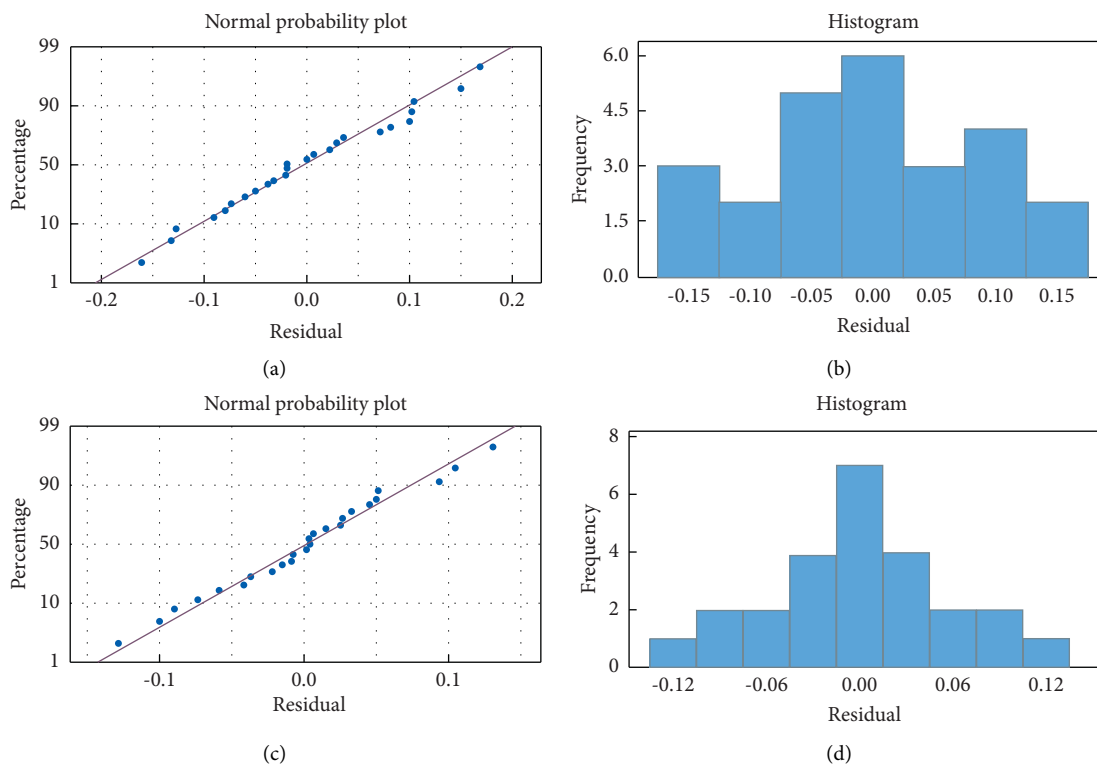


FIGURE 9: Analysis results of model II. (a) Normal probability plot ($925 \leq (t) \leq 980$). (b) Histogram ($925 \leq (t) \leq 980$). (c) Normal probability plot ($990 \leq (t) \leq 1025$). (d) Histogram ($990 \leq (t) \leq 1025$).

TABLE 7: Process parameters of test samples.

Sample	T	D	S
1	925	70	1000
2	950	40	300
3	975	60	100
4	1000	50	100
5	1025	50	500

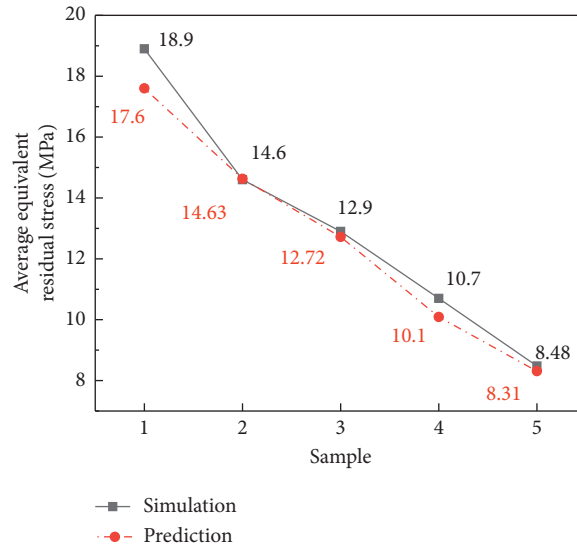


FIGURE 10: Comparison between simulated data and predicted data.

solve the two regression models. The results are shown in Figures 8 and 9.

The regression models obtained after calculation are as follows:

$$\begin{aligned}
 \text{Model I : } & \left\{ \begin{aligned} \sigma &= -0.11233t + 0.02085 d - 0.001276s + 121.16 & (925 \leq t \leq 980) \\ \sigma &= -0.06263t + 0.0336 d - 0.000721s + 71.13 & (990 \leq t \leq 1025) \end{aligned} \right\}, \\
 \text{Model II : } & \left\{ \begin{aligned} \sigma &= e^{(-0.00773t+0.00181 d-0.000087s+9.98)} & (925 \leq t \leq 980) \\ \sigma &= e^{(-0.00661t+0.00358 d-0.000073s+8.75)} & (990 \leq t \leq 1025) \end{aligned} \right\},
 \end{aligned} \tag{4}$$

where $t \in [925, 980] \cup [990, 1025]$, $d \in [40, 70]$, and $s \in [100, 1000]$.

By comparing Figures 8 and 9, it can be seen that the normalized residual of regression model II is closer to the normal distribution and has higher accuracy. Therefore, regression model II was selected as the prediction model of the average equivalent residual stress.

4.2. Model Validation. Since the simulation model has been modified by experiments, it can be used to verify the accuracy of the prediction model. Another 5 sets of forging process parameters were selected as test samples for simulation and model prediction, as shown in Table 7. The comparison result is shown in Figure 10, from which it can be seen that the simulation data are very close to the predicted data and the error is small. This indicates that the

prediction model can accurately reflect the mapping relationship between the forging process parameters and the average equivalent residual stress of Ti-6Al-4V alloy forgings. It also indicates that the prediction model can effectively guide the prediction of the residual stress of Ti-6Al-4V alloy forgings in practical engineering.

5. Conclusions

By using the modified finite element model, the primary and secondary relationship of key factors affecting the average equivalent residual stress of Ti-6Al-4V alloy forgings was analyzed and the optimal process parameters with minimum residual stress were obtained. Then, the multiple linear regression analysis was carried out based on the simulation data, and the mathematical model which can effectively

predict the average equivalent residual stress was determined. The significant conclusions have been drawn below:

- (1) In nonisothermal forging, the deformation temperature is the main factor affecting the residual stress of the forging, followed by the degree of deformation, and the deformation speed has the least influence on the residual stress of the forging.
- (2) The optimal combination of process parameters for the minimum residual stress of forgings without considering mechanical properties is deformation temperature 1025°C, deformation degree 30%, and deformation speed 1000 mm/s. For the parts that require high-dimensional stability but not too much mechanical properties, this optimal combination of process parameters has certain reference significance.
- (3) In the regression analysis, according to the distribution characteristics of the residual stress of Ti-6Al-4V alloy forgings in the upper and lower regions of the transformation point (985°C), the regression model was divided into two temperature regions, which can accurately reflect the mapping relationship between the key process parameters and the average equivalent residual stress.

Data Availability

The data used to support the findings of this study are included within the article.

Conflicts of Interest

The authors declare that they have no conflicts of interest.

Acknowledgments

The authors gratefully acknowledge the financial support of this study by the National Natural Science Foundation of China (Grant no. 51775427).

References

- [1] X. Fang, J. Wu, X. Ou, and F. Yang, "Microstructural characterization and mechanical properties of Ti-6Al-4V alloy subjected to dynamic plastic deformation achieved by multipass hammer forging with different forging temperatures," *Advances in Materials Science and Engineering*, vol. 2019, Article ID 6410238, 12 pages, 2019.
- [2] J. C. Williams and R. R. Boyer, "Opportunities and issues in the application of titanium alloys for aerospace components," *Metals - Open Access Metallurgy Journal*, vol. 10, no. 6, 2020.
- [3] H. M. Nu, T. T. Le, L. P. Minh, and H. L. Nguyen, "A study on rotary friction welding of titanium alloy (Ti6Al4V)," *Advances in Materials Science and Engineering*, vol. 2019, Article ID 4728213, 9 pages, 2019.
- [4] W. Rae, "Thermo-metallo-mechanical modelling of heat treatment induced residual stress in Ti-6Al-4V alloy," *Materials Science and Technology*, vol. 2019, p. 20, 2019.
- [5] M. Pérez, "Microstructural evolution of Nimonic 80a during hot forging under non-isothermal conditions of screw press," *Journal of Materials Processing Technology*, vol. 252, pp. 45–57, 2018.
- [6] S. Yang, H. Li, J. Luo, Y.-G. Liu, and M.-Q. Li, "Prediction model for flow stress during isothermal compression in $\alpha+\beta$ phase field of TC4 alloy," *Rare Metals*, vol. 037, no. 5, pp. 369–375, 2018.
- [7] Y. Kim, Y. B. Song, S. H. Lee, and Y. Kwon, "Characterization of the hot deformation behavior and microstructural evolution of Ti-6Al-4V sintered preforms using materials modeling techniques," *Journal of Alloys and Compounds*, vol. 675, pp. 15–25, 2016.
- [8] C. Garcia, T. Lotz, M. Martinez, A. Artemev, R. Alderliesten, and R. Benedictus, "Fatigue crack growth in residual stress fields," *International Journal of Fatigue*, vol. 87, pp. 326–338, 2016.
- [9] F. Jamal, K. Mohamed, S. Amira, B. Samuel, E. Riadh, and J. Frédéric, "Impact of residual stresses on mechanical behaviour of hot work steels," *Engineering Failure Analysis*, vol. 94, pp. 33–40, 2018.
- [10] D. L. Ball, "An update on the impact of forging residual stress in airframe component design," *Materials Performance and Characterization*, vol. 7, no. 4, pp. 827–861, 2018.
- [11] Z. Bi, H. Qin, Z. Dong, X. Wang, and Ji Zhang, "Residual stress evolution and its mechanism during the manufacture of superalloy disk forgings," *Acta Metallurgica Sinica*, vol. 55, no. 9, pp. 1160–1174, 2019.
- [12] M. Araghchi, H. Mansouri, R. Vafaei, and Y. Guo, "Optimization of the mechanical properties and residual stresses in 2024 aluminum alloy through heat treatment," *Journal of Materials Engineering and Performance*, vol. 27, no. 7, pp. 3234–3238, 2018.
- [13] J. S. Robinson, D. A. Tanner, and S. V. Petegem, "Influence of quenching and aging on residual stress in Al-Zn-Mg-Cu alloy 7449," *Materials Science and Technology*, vol. 28, no. 4, pp. 420–430, 2012, <https://www.tandfonline.com/author/Evans%2C+A>.
- [14] Y. B. Dong, W. Z. Shao, J. T. Jiang, B.-Y. Zhang, and L. Zhen, "Minimization of residual stress in an Al-Cu alloy forged plate by different heat treatments," *Journal of Materials Engineering and Performance*, vol. 24, no. 6, pp. 2256–2265, 2015.
- [15] F. O. Neves, T. Oliveira, D. U. Braga, and A. Chaves da Silva, "Influence of heat treatment on residual stress in cold-forged parts," *Advances in Materials Science and Engineering*, vol. 2014, Article ID 658679, 6 pages, 2014.
- [16] N. Karunathilaka, N. Tada, T. Uemori et al., "Effect of lubrication and forging load on surface roughness, residual stress, and deformation of cold forging tools," *Metals - Open Access Metallurgy Journal*, vol. 9, no. 7, 2019.
- [17] A. Ameli and M. R. Movahhedy, "A parametric study on residual stresses and forging load in cold radial forging process," *International Journal of Advanced Manufacturing Technology*, vol. 33, no. 1-2, pp. 7–17, 2007.
- [18] Y. Zhang and Y. Gao, "Study on residual stress of hot die forging for alloy GH4169 turbine disc based on DEFORM-2D," *Forging & Stamping Technology*, vol. 43, no. 03, pp. 1–7, 2018.
- [19] M. Kardan, A. Parvizi, and A. Askari, "Influence of process parameters on residual stresses in deep-drawing process with FEM and experimental evaluations," *Journal of the Brazilian Society of Mechanical Sciences and Engineering*, vol. 40, no. 3, pp. 1–12, 2018.
- [20] X. Fang, Y. Shao, and J. Lu, "Influence of forging process parameters on residual stress of TC4 titanium alloy forgings," *Forging & Stamping Technology*, vol. 46, no. 3, pp. 1–8, 2021.
- [21] T. Ram Prabhu, "Simulations and experiments of the non-isothermal forging process of a Ti-6Al-4V impeller," *Journal*

- of Materials Engineering and Performance*, vol. 25, no. 9, pp. 3627–3637, 2016.
- [22] X. Fang, J. Lu, J. Wang, and J. Yang, “Parameter optimization and prediction model of induction heating for large-diameter pipe,” *Mathematical Problems in Engineering*, vol. 2018, Article ID 8430578, 12 pages, 2018.
- [23] Y. Wang and X. Huo, “Multiobjective optimization design and performance prediction of centrifugal pump based on orthogonal test,” *Advances in Materials Science and Engineering*, vol. 2018, Article ID 6218178, 10 pages, 2018.
- [24] N. H. Alharthi, B. Sedat, A. T. Abbas, M. Aly, and H. Alharbi, “Prediction of cutting conditions in turning AZ61 and parameters optimization using regression analysis and artificial neural network,” *Advances in Materials Science and Engineering*, vol. 2018, Article ID 1825291, 10 pages, 2018.
- [25] S. K. Madhavi, S. Hanuman, and R. U. Rao, “Regression model developed using RSM for predicting withstanding pressure of HDPE pipe during extrusion process,” *Recent Advances in Material Sciences Select Proceedings of ICLJET 2018*, vol. 8, pp. 177–185, 2019.
- [26] I. Gkioulekas and L. G. Papageorgiou, “Piecewise regression analysis through information criteria using mathematical programming,” *Expert Systems with Applications*, vol. 121, pp. 362–372, 2019.